Annals of 3D Printed Medicine 12 (2023) 100121

Contents lists available at ScienceDirect

Annals of 3D Printed Medicine

journal homepage: www.elsevier.com/locate/stlm

Research paper

Feasibility of additively manufacturing synthetic bone for sports personal protective equipment applications

Gemma Leslie [a,*], Keith Winwood [b], Andy Sanderson [c], Peter Zioupos [d], Tom Allen [a]

[a] Department of Engineering, Manchester Metropolitan University, Manchester M1 5GD, UK
[b] Department of Life Sciences, Manchester Metropolitan University, Manchester M1 5GD, UK
[c] Department of Sports and Exercise, Manchester Metropolitan University, Manchester M1 5GD, UK
[d] Department of Engineering, University of Hull, Kingston upon Hull HU6 7RX, UK

ARTICLE INFO

Keywords:
Bone surrogate
Radius
3-point bending
Cortical bone
Fused filament fabrication
Biofidelic

ABSTRACT

Human limb surrogates, of varying biofidelity, are used in the performance assessment of sports personal protective equipment (PPE). Such biofidelic surrogates have incorporated soft tissue simulants (silicones) and synthetic bone (short fibre filled epoxy). Testing surrogates incorporating realistic synthetic bone could help to further our knowledge of fracture trauma mechanics, and applications such as the effectiveness of sports PPE. Limb surrogates with embedded synthetic bone are rarely tested to fracture, mainly due to the effort and cost of replacing them. This paper proposes additive manufacturing of synthetic bones, with appropriate bone like fracture characteristics, potentially making them more accessible and cost effective. A Markforged® X7™ printer was used as it prints a base filament (Onyx™) alongside a continuous strand of reinforcement (e.g., carbon fibre). The properties of specimens from this printer vary with the type, volume fraction and position of reinforcement. Bar specimens (10 × 4 × 120 mm) with varying amounts of carbon fibre reinforcement were printed for three-point bend testing to determine the feasibility of achieving mechanical properties close to compact bone (bending modulus of ~15 GPa, bending strength of ~180 MPa). Bending strength for the various bar specimens ranged from 32 to 378 MPa, and modulus values ranged from 1.5 to 25.8 GPa. Based on these results, four 140 mm long oval shaped cylindrical specimens of ø14 and ø16 mm were printed to represent a basic radius bone model. Three-point bend testing of these bone models showed similar bending modulus (3.8 to 5.3 GPa vs. 3.66 to 14.8 GPa) to radius bones reported in the literature, but higher bending strength (147 to 200 MPa vs. 80.31 ± 14.55 MPa).

Introduction

Human limb surrogates are used to assess the performance of sports personal protective equipment (PPE), such as wrist protectors, shin guards and thigh pads [1]. These surrogates often consist of simplified geometries and stiff materials, such as a metal hemisphere or hemi-cylinder, that only offer a basic representation of human anthropometry. These basic surrogates are well suited to certification tests performed within test houses (e.g., EN 13,061:2009, EN 20,302:2020, BS 6183–3:2000), as they offer a low cost, simple and repeatable solution [2]. Recent work has improved the biofidelity (modelling the biological response) of human limb surrogates by utilising soft tissue simulants and synthetic bone [1–3]. Such improvements in human limb surrogates are arguably crucial in the development, testing and certification of more effective sports PPE [4].

Payne et al. [1,5] developed a thigh surrogate consisting of a synthetic femur (Sawbones®, Washington State, US) with multi-material simulants replicating soft tissues within the thigh. The surrogate was used to assess impact response of a cricket ball at 24 J. Ankrah and Mills [6] developed a lower leg surrogate consisting of a Sawbones® synthetic tibia surrounded with soft tissue simulant. This was used to assess football shin guards via stud impacts up to 5 J. According to the authors of these studies, the surrogates (both thigh and lower leg) offered a more biofidelic response than the fixed metal anvils typically used in certification tests. They provided data on acceleration and surface strain of the thigh, and pressure distribution under a shin guard. However, neither of these surrogates were tested in a manner that led to bone fracture, and thus this failure mechanism was not studied. The reason they were not

* Corresponding author.
E-mail address: gemma.leslie@manchester.ac.uk (G. Leslie).

https://doi.org/10.1016/j.stlm.2023.100121
Received 29 June 2023; Accepted 9 August 2023

tested at fractious impact energies was most likely to prevent damage in test equipment [6] and perhaps for the cost and effort of replacing the synthetic bone and remaking the surrogate.

Recent work of ours investigated the effect of adding a soft tissue simulant (an outer layer of silicone) to a wrist surrogate for testing wrist protectors [2,7]. Adding the soft tissue simulant stiffened the surrogate-protector system during a bend test [2] and reduced peak force in an impact test [7]. Incorporating a biofidelic frangible synthetic bone into such a wrist surrogate would, in this instance, augment further the biofidelic nature of the wrist/wrist protector complex. It would also add another level of scientific knowledge on the wrist injury mechanism and the efficacy of wrist protection, and provide a method for optimising the protective elements themselves (pads, splints).

Commercial synthetic bones, e.g., Sawbones®, are typically made from short fibre filled epoxy and validated against the quasi-static properties of cadaveric human bone. Additive manufacturing is becoming increasingly accessible and is being driven by the development of new printable materials and associated processes [8]. There are also human bone geometries available for additive manufacturing (i.e., from computerised tomography scans and embodi3D® (Washington, USA)). Such geometries become useful for testing if they can be printed in materials that provide mechanical properties representative of bone. If the printer settings to give specific properties were available alongside such bone geometries, researchers and practitioners could print them for their intended applications. Furthermore, such synthetic bones could be tailored for a specific application, or demographic characteristics (e.g. ageing models or osteoporosis with increased levels of porosity), by adjusting the geometry and print settings.

Chong et al. [9] and Heiner [10] tested the quasi-static properties of human cortical bone (compressive strength and modulus – 170 MPa, 17 GPa, tensile strength and modulus – 130 MPa, 17 GPa) alongside those of a Sawbone® femur and tibia. The mechanical properties of Sawbones® cortical bone (short fibre filled epoxy) were: a compressive strength and modulus of 157 MPa and 17 GPa, respectively, and a tensile strength and modulus of 106 MPa and 16 GPa, respectively. Other studies have tested the bending strength and modulus of human cortical bone, with values ranging from 104 to 238 MPa and 9 to 19 GPa, respectively [11–14]. Consequently, validation studies for commercially available synthetic bones are typically based on human femur and tibia bones. There are few studies on the mechanical properties of upper extremity bones, such as the radius and ulna, which would be required for a wrist surrogate [15–17]. Weerasooriya et al. [18] state the mechanical properties of bones are unique to the specific bone and should not be generalised for the whole skeleton.

The mechanical properties of human radius bones have been reported as; 207 to 212 MPa for bending strength and 16 GPa for bending modulus [19], 33 to 178 MPa for compressive strength and 10 to 19 GPa for compressive modulus [15,20,21]. Singh et al. [16] conducted three-point bend testing of three cadaveric radius bones (age 45 to 55 years), reporting (mean and standard deviation) bending strength of 80.31 ± 14.55 MPa, bending modulus of 3.66 ± 0.78 GPa, and bending stiffness of 0.7 ± 0.02 kN/mm. These values by Singh et al. [16] are lower than those reported by Motoshima [19], although the former noted that the latter did not state storage conditions nor loading rates. Similarly, Ketsiri et al. [17] conducted three-point bend testing of cadaveric radius bones (age 72 ± 8 years) to develop a finite element model with suitable estimates of the modulus (9.42 ± 2.13 GPa) and yield stress (140.72 ± 34.93 MPa). Force displacement graphs for four cadaveric radius bones were reported, with fracture force ranging from ~700 to 2600 N.

Fused filament fabrication (FFF) is an established method of additive manufacturing [22], allowing printing of Polylactic acid (PLA) and Acrylonitrile Butadiene Styrene (ABS). These two printed materials have a bending modulus of ~3 GPa and a bending strength of ~70 MPa,[1] both lower than values reported for human bone. ABS has been used to print models of human skulls and spinal segments [23–25]. Despite ABS having a lower Young's modulus than cortical bone (~3 vs. ~10–20 GPa), the force displacement curves for the printed specimens were similar to cadaveric ones in the elastic region. Pullen et al. [26] assessed 12 common print filaments (including ABS and PLA) to determine their suitability in vertebral models. None of the filaments were deemed comparable to cortical bone, due to their lower density, although Polyethylene terephthalate glycol (PETG) and Chlorinated polyethylene (CPE) were close to cancellous and mineral bone standard.

Some 3D printers, such as those of Markforged® (Massachusetts, USA), offer continuous fibre fabrication. These printers combine FFF with a second extruder that deposits a continuous strand of reinforcement to give a composite material. The base material of Markforged®, Onyx™ (micro carbon fibre filled polyamide), has a similar Young's modulus to PLA and ABS of ~3 GPa[2] and is hence also more compliant than human bone. When Onyx™ is combined with reinforcement, including carbon fibre with a Young's modulus of ~50 GPa[2], a stiffer composite material can be produced. Onyx™ has a similar bending strength to PLA and ABS (~71 MPa), with much higher values for carbon fibre of 540 MPa[2]. As such, by combining Onyx™ with a reinforcement, such as carbon fibre, it may be possible to recreate the mechanical properties of cortical bone (i.e., bending strength of ~180 MPa, bending modulus of ~15 GPa [16,17,19]) more closely than printing materials like PLA and ABS alone.

The present study explores the feasibility of additively manufacturing a synthetic radius bone to advance further the development of a biofidelic limb surrogate for assessing wrist protectors [2,7]. The aim is to determine the feasibility of using the Markforged® Onyx™ and carbon fibre filament to print a synthetic radius bone with similar mechanical properties (bending strength and modulus) to those reported in the literature for human radius bones.

Method

Sample printing

A total of 21 three-point bend test bar specimens (10 × 4 × 120 mm, as per ASTM D790–17) were printed in Onyx™ (base filament) and carbon fibre (reinforcement filament) on a Markforged® X7™. Carbon fibre was chosen as the stiffest available reinforcement (carbon FR, Kevlar®, fibreglass, HSHT fibreglass)[2]. Print parameters (amount of reinforcement, reinforcement type, and infill) were set in the accompanying software (Eiger™). The amount of reinforcement fibre was varied between specimens and printed using either the concentric or isotropic fill type. Concentric fill lays fibre around the perimeter of a wall (Fig. 1a), and the number of fibre rings can be specified. Isotropic fill routes fibre back and forth along the part (Fig. 1b and c). Isotropic fibre layers are typically rotated by 45° between layers, however this method was used to set the fibres to lay along either the length (Fig. 1b) or width (Fig. 1c) of the part (either at 0 or 90° depending on the position of the print bed).

Three of each of the specimens in Table 1 were printed (total $n = 21$). The reinforcement percentage relates to the amount of base reinforcement layers to base layers. Each specimen had ~40 printed layers in total, so 91% reinforcement meant ~36 layers of reinforcement (due to the base filament wall thickness and geometry of the sample, 100% reinforcement is unattainable or unsuitable). The wall thickness for each specimen was set to two layers, giving four in total through the

[1] Reported values according to the Ultimaker datasheet (Utrecht, Netherlands).

[2] Reported values according to the supplier datasheet (Markforged®).

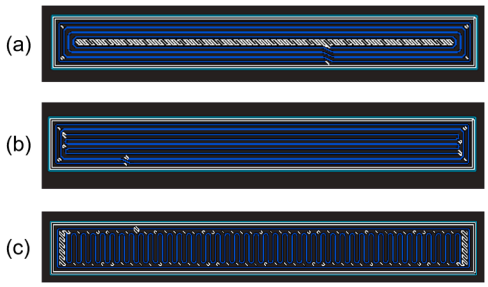

Fig. 1. Types of fibre fill for the 10 × 4 × 120 mm bar specimens. (a) concentric with two rings, (b) isotropic along length, (c) isotropic along width (blue lines indicate fibre). Images generated by the additive manufacturing printer's software (Eiger™) based on settings selected.

Table 1
Printing parameters of the 10 × 4 × 120 mm Onyx™ and carbon fibre bar specimens.

Reinforcement Fill Type	Number of Rings (concentric)/Angle of fibres (isotropic)	Reinforcement Percentage (%)	Infill (%)
Concentric	2	78	35
	3	91	100
Isotropic length	90	56	35
	90	78	100
Isotropic width	0	56	35
	0	78	100
None	–	0	100

thickness. The infill is the internal structure of the base material. Infill was set as triangular when <100%. One specimen was printed without reinforcement and with 100% infill for comparison.

Synthetic bone samples

To represent a simple uniform bone shape, oval cylinder specimens were printed. The 'oval' shape (Fig. 2), achieved by applying a ⌀5 mm fillet and ⌀8 mm fillet to opposite sides of a 16 mm sided cuboid, created a flat surface on each side, which was more stable on the print bed, and thus the print quality was better than for a true oval cylinder. Two pairs of synthetic bone specimens were printed, one pair with a diameter of 14 mm and the other 16 mm, all 140 mm long. As the cross-section dimensions of the cadaveric bones tested in the literature were not stated, the diameters of the synthetic ones were related to those of the large Sawbones® radius.[3] The print settings for the bones were based on the results from the bar specimen tests (see Results Section).

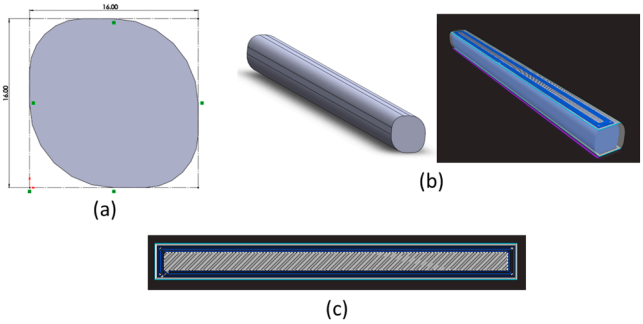

Fig. 2. Synthetic bone specimen (⌀16 mm) (a) cross-section, (b) isometric view of outer geometry (left) and internal reinforcement (right), (c) internal top view showing the reinforcement placement (blue lines indicate reinforcement). Dimensions in mm.

Three-point bend method

Three-point bend tests were performed on a uniaxial test machine (Hounsfield HK10S, Tinius Oslen, Surrey, UK) fitted with either a 1 or 10 kN load cell (for bar or synthetic bone specimens) (Fig. 3). The test procedure for the bar specimens (Fig. 3a) followed ASTM D790–17. The support span length was 64 mm, equating to 16 times the 4 mm depth of the bars. Specimens were tested to fracture or to a displacement of 12 mm (corresponding to the maximum possible on the test rig). Test speed ranged from 5 to 500 mm/min. Force vs. displacement was recorded at a sample rate of 6 Hz. Stress and strain are those of the outer layers as per linear elastic analysis [27], and calculated as per ASTM D790–17 (using the span length and specimen dimensions).

The test procedure for the synthetic bone specimens (Fig. 3b) followed those of Ketsiri et al. [17] and Singh et al. [16], facilitating comparisons. One set (one ø14 mm, one ø16 mm) of synthetic bone specimens were tested at 6.5 mm/min with a span length of 98 mm, as per Ketsiri et al. [17]. The other two bones were tested at 1 mm/min, with a span length of six times the diameter (84 and 96 mm), as per Singh et al. [16]. The synthetic bone specimens were tested in the orientation of Fig. 2b. Ketsiri et al. [17] noted their cadaveric bone specimens were positioned with the anterior surface down, whereas Singh et al. [16] did not report the test orientation. Force vs. displacement was recorded, stress and strain [27] were calculated as per ASTM D790–17, and bending strength, bending modulus, strain at fracture, bending stiffness, and yield stress were calculated from either the force-displacement or stress-strain data.

Results

Density of the various 10 × 4 × 120 mm bar specimens ranged from 1031 to 1282 kg/m^3. The various bar specimens covered a range of bending strength, bending modulus, strain at fracture and stiffness values (Table 2 and Fig. 4). The bending strength and modulus of the bars ranged from 32 to 378 MPa and 8.1 to 21.8 GPa, respectfully. The bars with isotropic length reinforcement had the highest bending strength and modulus, exceeding those in the literature for human cortical bone (bending strength ~180 MPa, bending modulus ~15 GPa [16,17,19]), whereas those with isotropic width reinforcement produced the lowest values, below those reported in the literature. The specimens with concentric reinforcement, 91% reinforcement and 100%

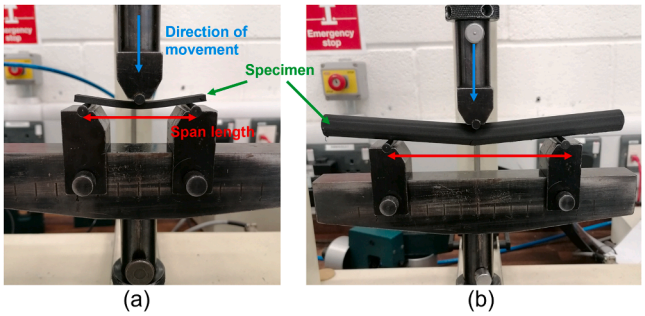

Fig. 3. Three-point bend test setup for (a) bar specimens and (b) synthetic bone specimens.

[3] Sawbones® biomechanical products catalogue states a diameter of 16 mm

Table 2
Bending properties of the 10 × 4 × 120 mm bar specimens with varying amounts of carbon fibre to Onyx™ filament and different fill types.

Reinforcement Fill Method	Strength (MPa)	Bending Modulus (GPa)	Strain at Fracture (%)
No reinforcement	30–38	0.8–1.0	> 6
Concentric	143–249	8.1–13.0	2 - 3
Isotropic length	271–378	15–21.8	2 - 3
Isotropic width	32–51	1.5–2.0	> 6
Human cortical bone [16, 17,19]	~180	~15	–

infill had bending strength and modulus values closest to those for human cortical bone (Fig. 4a). As such, the concentric reinforcement method (three concentric rings, ~80% reinforcement, wall thickness two layers, 100% infill) was used for printing the four synthetic bone specimens (Fig. 2).

The density of the 14 and 16 mm diameter synthetic bone specimens was 1348 and 1250 kg/m^3, respectively. The density of the human radius bones from literature were unreported, however, the densities reported here are similar to Sawbone® cortical bone (1640 kg/m^3) and those of human femurs tested by Keller et al. [12] (1.311 to 1.718 kg/m^3). The bending properties of the synthetic bone specimens were similar to those reported elsewhere for human radius bone (Tables 3 and 4). The bending modulus of the 14 mm diameter synthetic bones, and the yield stress of both sized synthetic bones lay within the range reported by Ketsiri et al. [17] (Table 3). The bending modulus value of both sized synthetic bones lay within the range reported by Singh et al. [16]. Ketsiri et al. [17] showed the variety between cadaveric human radius bones (with fracture force ranging from ~700 to 2600 N), and the gradient of the force-displacement curve, and hence stiffness, for the synthetic bones, was closest to the two examples in Fig. 5, particularly below 2 mm displacement. Due to the age range of cadavers tested by Ketsiri et al. [17] (age 72 ± 8 years), there may be differences in porosity and modulus, and furthermore, other influential factors of cadaveric studies such as diet, lifestyle, genetics and ethnicity contribute to differences within material and mechanical properties. The synthetic bone samples had a higher bending strength than both of these human radius bones (Fig. 5).

Discussion

Biofidelic human limb surrogates (physical models) are invaluable in the development, testing and certification of sport PPE. In this study a combination of Onyx™ and carbon fibre reinforcement was used to print synthetic radius bones with similar mechanical properties to those reported in the literature for human radius bones. Bar specimens (10 × 4 × 120 mm) of varying amounts of Onyx™ and carbon fibre reinforcement achieved mechanical properties similar to cortical bone [11–14, 19]. Bending strength values of 32 to 378 MPa and bending modulus values of 1.5 to 27.8 GPa were achieved (Table 2), which covered the target values of cortical bone from the literature (bending strength of ~180 MPa, bending modulus of ~15 GPa [16,17,19]). This result suggested that the mechanical properties of cortical bone, in terms of bending strength and modulus, could be achieved at the material level, using this additive manufacturing method and filaments. The concentric fill reinforcement method produced bars with bending properties closer to the human cortical bone than the isotropic fill method. As such, a concentric fill was used when printing simplified synthetic bone specimens.

Oval shaped cylinder specimens of 14 and 16 mm diameter (140 mm length), based on that of the large Sawbone® radius, were printed as a basic representation of a human radius bone. These specimens were tested following the methods of Ketsiri et al. [17] and Singh et al. [16]. When tested according to Ketsiri et al. [17], the bending modulus value of 5.3 GPa for the 14 mm synthetic bone was towards the lower end of

Table 3
Three-point bending properties of the Onyx™ and carbon fibre synthetic bone specimens, following the test procedure of Ketsiri et al. [17].

Sample	16 mm diameter	14 mm diameter	Ketsiri et al. [17]
Bending strength (MPa)	199.5	175.2	–
Bending Young's modulus (GPa)	4.1	5.3	5.16 to 14.48
Bending stiffness (kN/mm)	1.04	0.83	–
Yield stress (MPa)	~180	~150	60.87 to 226.97

Table 4
Three-point bending properties of the Onyx™ and carbon fibre synthetic bone specimens, following the test procedure of Singh et al. [16].

Sample	16 mm diameter	14 mm diameter	Singh et al. [16]
Bending strength (MPa)	185.3	146.9	80.31 ± 14.55
Bending Young's modulus (GPa)	4.1	3.8	3.66 ± 0.78
Bending stiffness (kN/mm)	1.22	1.03	0.7 ± 0.02

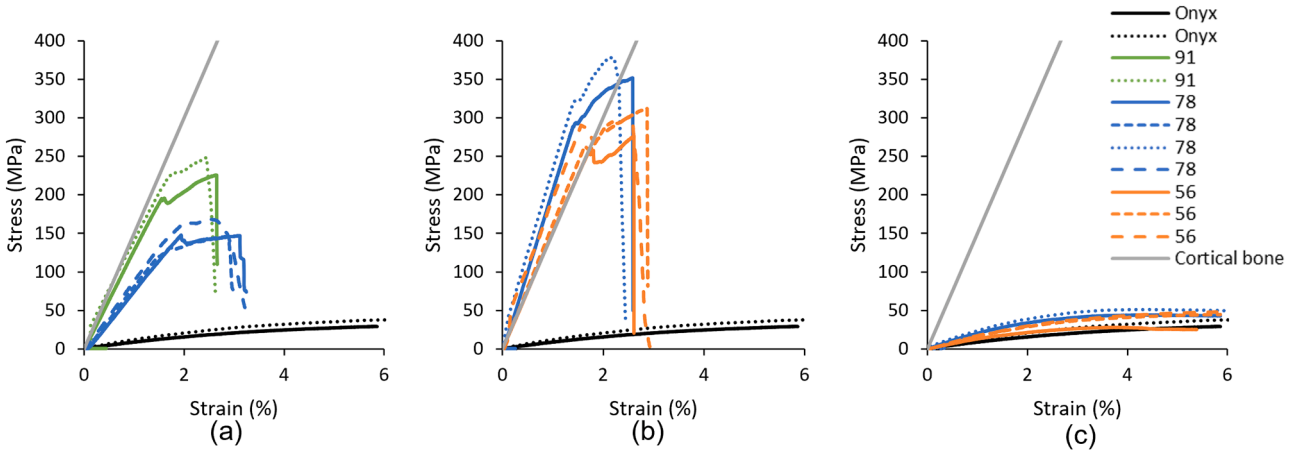

Fig. 4. Stress strain relationship [26] of the various bar specimens of varying reinforcement percentage tested with (a) concentric fibre fill, (b) isotropic length fibre fill, (c) isotropic width fibre fill (solid line represent 5 mm/min test speed, short dashed 50 mm/min, dotted lines 300 mm/min, long dashed lines 500 mm/min). The straight line representing cortical bone is based on the Young's modulus reported by Motoshima [19].

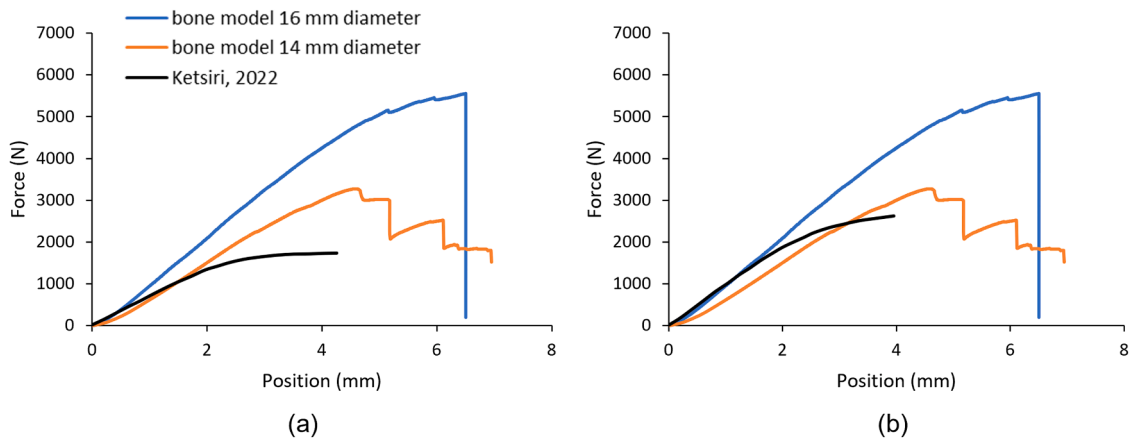

Fig. 5. Force displacement relations of the synthetic bone model specimens compared to the digitised results from Ketsiri et al. [17].

the values they reported (5.16 to 14.48 GPa) (Table 3). Furthermore, the respective yield stress of ~180 and ~150 MPa for the 16 and 14 mm diameter synthetic bones lay within the range reported by Kitsiri et al. [17] (60.87 to 226.97 MPa). When tested according to Singh et al. [16], the respective bending modulus values of 4.1 and 3.8 GPa for the 16 and 14 mm diameter synthetic bones were within the range they reported (3.66 ± 0.78 GPa) (Table 4). The force displacement relationship of both sized synthetic bones were also comparable with two of the examples from Ketsiri et al. [17] (Fig. 5), particularly at low displacement, but with higher bending strength. Overall, the material properties reported for the printed bones were closer to those of human bone than those of the metal anvils typically used for PPE certification testing.

This work is limited to quasi-static testing of synthetic bone specimens with a basic shape. Whilst this enabled comparison with literature loading cadaveric human bones slowly, the results may not necessarily translate to dynamic scenarios that relate to falls and impacts [28]. Future work could therefore test in comparison commercial and additively manufactured synthetic bones at higher loading rates. Another limitation was the reinforcement fill types available for printing specimens. The concentric and isotropic methods only allow selection of which layers to add reinforcement, rather than specific areas within them. Only two (one ø14 mm, one ø16 mm) synthetic bone specimens were tested for comparison with each of the published studies [16,17]. Future work could test more synthetic bone specimens to gauge printing consistency, and furthermore, trying the other reinforcement filaments available.

The geometry of the synthetic bone specimens was simplified in shape with a uniform cross-section, which is not the case for bone tissue. Variation within shape also alters with age from children to adults and porosity values during ageing and certain disease states such as osteoporosis. As such, factors such as shape and porosity in relation to age specific may be beneficial for future testing. Furthermore, due to limited detail in the literature testing cadaveric radius bones, it was not possible to ensure the test orientation of the printed specimens matched those used for validating them. Future work could use more representative geometries for bones, such as those from computerised tomography scans or available computer aided design geometries. The parameters used here to print the synthetic bones (concentric fill reinforcement with three concentric rings, reinforcement of ~80%, wall thickness 2 layers, 100% infill) produced similar three-point bend test results to both Ketsiri et al. [17] and Singh et al. [16], and fine tuning of these could further improve results. This could include tuning the printing parameters to match compressive and tensile properties to desired values, or tailoring for a specific application or demographic. Furthermore, torsional testing could be considered. For example, Heiner [10] reported the torsional properties of cadaveric and synthetic (Sawbone®) tibia and femur bones, which could be compared against results from torsional testing of 3D printed bone specimens.

The synthetic bone specimens in this study only represented cortical bone values. This would replicate the diaphysis (mid-shaft) section of the radius where there is very little cancellous/trabecular bone. Therefore, future work could include the mechanical properties of trabecular bone to mimic the areas of the epiphysis and metaphysis where wrist fractures are predominantly present. Future work could also look to print a synthetic soft tissue layer alongside the synthetic bone [29]. Such an approach could potentially enable a consistent, accessible and cost effective way to make a biofidelic limb surrogate via additive manufacturing.

Conclusion

Additively manufacturing three-point bend test bar specimens with various amounts of carbon fibre reinforcement and Onyx™ as base material, achieved mechanical properties covering the values reported within the published literature for human cortical bone. Synthetic bones of simple uniform shape, with ~80% carbon fibre concentric fill and 100% infill, produced similar values of bending modulus and higher values of bending strength, as reported in the literature for testing of cadaveric human radius bones.

Declaration of Competing Interest

The authors declare that they have no known competing financial interests or personal relationships that could have appeared to influence the work reported in this paper.

Funding

This research was internally funded by the Musculoskeletal Science and Sports Medicine (MSSM) research centre at Manchester Metropolitan University.

Acknowledgments

We would like to thank the Musculoskeletal Science and Sports Medicine (MSSM) research centre and Manchester Metropolitan University for funding the research, and PrintCity for their assistance in printing the specimens.

References

[1] Payne T, Mitchell S, Halkon B, Bibb R, Waters M. Development of a synthetic human thigh impact surrogate for sports personal protective equipment testing. In: Proceedings of the Institution of Mechanical Engineers. Part P: Journal of Sports

Engineering and Technology. 230; 2016. p. 5–16. https://doi.org/10.1177/1754337115582294.
[2] Leslie G, Wang W, Winwood K, Liauw C, Hamilton N, Allen T. Effect of surrogate surface compliance on the measured stiffness of snowboarding wrist protectors. In: Proceedings of the MDPI; 2020. p. 49. https://doi.org/10.3390/proceedings2020049084.
[3] Imam SA, Hughes AC, Carré MJ, Driscoll H, Winwood K, Venkatraman P, Allen T. Finite element model to simulate impact on a soft tissue simulant. Sports Eng 2023;26:16. https://doi.org/10.1007/s12283-023-00407-7.
[4] Payne T, Mitchell S, Bibb R, Waters M. Initial validation of a relaxed human soft tissue simulant for sports impact surrogates. Procedia Eng 2014;72:533–8. https://doi.org/10.1016/j.proeng.2014.06.092.
[5] Payne T. Improved human soft tissue thigh surrogates for superior assessment of sports personal protective equipment (Doctoral dissertation, Loughborough University). 2015.
[6] Ankrah S, Mills NJ. Performance of football shin guards for direct stud impacts. Sports Eng 2003;6(4):207–19. https://doi.org/10.1007/BF02844024.
[7] Leslie GE, Winwood K, Wang W, Hamilton N, Allen T. Effect of limb surrogate surface compliance on the impact response of wrist protectors. JSAMS Plus 2023;2:100023. https://doi.org/10.1016/j.jsampl.2023.100023.
[8] Chua CK, Yeong WY, An J. 3D printing for biomedical engineering. Materials 2017;10(3):243. https://doi.org/10.3390/ma10030243 (Basel).
[9] Chong A.C., Miller F., Buxton M., Friis E.A. Fracture toughness and fatigue crack propagation rate of short fibre reinforced epoxy composites for analogue cortical bone. 2007:487–93. 10.1115/1.2746369.
[10] Heiner AD. Structural properties of fourth-generation composite femurs and tibias. J Biomech 2008;41(15):3282–4. https://doi.org/10.1016/j.jbiomech.2008.08.013.
[11] Currey JD. What determines the bending strength of compact bone? J Exp Biol 1999;202(18):2495–503. https://doi.org/10.1242/jeb.202.18.2495.
[12] Keller TS, Mao Z, Spengler DM. Young's modulus, bending strength, and tissue physical properties of human compact bone. J Orthop Res 1990;8(4):592–603. https://doi.org/10.1002/jor.1100080416.
[13] Sedlin ED, Hirsch C. Factors affecting the determination of the physical properties of femoral cortical bone. Acta Orthop Scand 1966;37(1):29–48. https://doi.org/10.3109/17453676608989401.
[14] Lotz JC, Gerhart TN, Hayes WC. Mechanical properties of metaphyseal bone in the proximal femur. J Biomech 1991;24(5):317–29. https://doi.org/10.1016/0021-9290(91)90350-V.
[15] Bosisio MR, Talmant M, Skalli W, Laugier P, Mitton D. Apparent Young's modulus of human radius using inverse finite-element method. J Biomech 2007;40(9):2022–8. https://doi.org/10.1016/j.medengphy.2010.03.009.
[16] Singh D, Rana A, Jhajhria SK, Garg B, Pandey PM, Kalyanasundaram D. Experimental assessment of biomechanical properties in human male elbow bone subjected to bending and compression loads. J Appl Biomater Funct Mater 2019;17(2). https://doi.org/10.1177/2280800018793816. 2280800018793816.
[17] Ketsiri T, Uppuganti S, Harkins KD, Gochberg DF, Nyman JS, Does MD. Finite element analysis of bone mechanical properties using MRI-derived bound and pore water concentration maps. Comput Methods Biomech Biomed Eng 2022:1–12. https://doi.org/10.1080/10255842.2022.2098016.
[18] Weerasooriya T, Sanborn B, Gunnarsson CA, Foster M. Orientation dependent compressive response of human femoral cortical bone as a function of strain rate. J Dyn Behav Mater 2016;2:74–90. https://doi.org/10.1007/s40870-016-0048-4.
[19] Motoshima T. Studies on the strength of bending of human long extremity bones. J Kyoto Pref. Med. Univ. 1960;68:1377–97.
[20] Yamada H., Evans F.G. Strength of biological materials. 1970.
[21] Louis O, Boulpaep F, Willnecker J, Van den Winkel P, Osteaux M. Cortical mineral content of the radius assessed by peripheral QCT predicts compressive strength on biomechanical testing. Bone 1995;16(3):375–9. https://doi.org/10.1016/8756-3282(94)00050-6.
[22] Singh S, Singh G, Prakash C, Ramakrishna S. Current status and future directions of fused filament fabrication. J Manuf Process 2020;55:288–306. https://doi.org/10.1016/j.jmapro.2020.04.049.
[23] Franceskides C, Leger T, Horsfall I, Tozzi G, Gibson M, Zioupos P. Evaluation of bone excision effects on a human skull model–I: mechanical testing and digital image correlation. In: Proceedings of the Institution of Mechanical Engineers. Part H: Journal of Engineering in Medicine. 234; 2020. p. 337–45. https://doi.org/10.1177/0954411919891885.
[24] Franceskides C, Arnold E, Horsfall I, Tozzi G, Gibson MC, Zioupos P. Spinal motion segments—I: concept for a subject-specific analogue model. J Bionic Eng 2020;17:747–56. https://doi.org/10.1007/s42235-020-0060-1.
[25] Stone B, Mitchell S, Miyazaki Y, Peirce N, Harland A. A destructible headform for the assessment of sports impacts. In: Proceedings of the Institution of Mechanical Engineers. Part P: Journal of Sports Engineering and Technology. 237; 2023. p. 7–18. https://doi.org/10.1177/17543371211055905.
[26] Pullen MW, Pooley RA, Kofler Jr JM, Valero-Moreno F, Ramos-Fresnedo A, Domingo RA, Perez-Vega C, Fox WC, Sandhu SJS, Quinones-Hinojosa A, Buchanan IA. A radiographic analysis of common 3D print materials and assessment of their fidelity within vertebral models. Ann 3D Print Med 2022;8:100080. https://doi.org/10.1016/j.stlm.2022.100080.
[27] Timoshenko Prof SP. X. On the transverse vibrations of bars of uniform cross-section. Lond Edinb Dublin Philos Mag J Sci 1922;43(253):125–31. https://doi.org/10.1080/14786442208633855. 1922.
[28] Greenwald RM, Janes PC, Swanson SC, McDonald TR. Dynamic impact response of human cadaveric forearms using a wrist brace. Am J Sports Med 1998;26(6):825–30. https://doi.org/10.1177/03635465980260061501.
[29] Jaksa L, Pahr D, Kronreif G, Lorenz A. Development of a multi-material 3D printer for functional anatomic models. Int J Bioprint 2021;7(4). https://doi.org/10.18063/ijb.v7i4.420.